



To what extent do physical measurements match with visual evaluation of soil structure?



Alice Johannes^{a,c,*}, Peter Weisskopf^b, Rainer Schulin^c, Pascal Boivin^a

^a University of Applied Sciences and Arts Western Switzerland hepia, Soils and Substrates Group, Institute Land-Nature-Environment, Route de Presinge 150, 1254 Jussy Geneva, Switzerland

^b Swiss Federal Research Station Agroscope, Soil Fertility and Soil Protection Group, Department of Natural Resources & Agriculture, Reckenholzstrasse 191, CH-8046 Zurich, Switzerland

^c Swiss Federal Institute of Technology ETH Zürich, Soil Protection group, Institute of Terrestrial Ecosystems, Universitätstrasse 16, 8092 Zürich, Switzerland

ARTICLE INFO

Article history:

Received 18 March 2016

Received in revised form 1 June 2016

Accepted 2 June 2016

Available online 16 June 2016

Keywords:

Soil structure

Shrinkage curve analysis

VESS

ABSTRACT

Soil structure quality can be scored by visual examinations or measured with soil physical properties. To investigate the relationships between these two approaches, we adapted the VESS (Visual Evaluation of Soil Structure, Guimarães et al., 2011) to the scoring of cores (CoreVESS) on which shrinkage analysis was also performed. Scoring was performed blindly after equilibrating the samples at -100 hPa matric potential and was compared to soil texture, soil organic carbon content (SOC), soil hydrostructural stability, structural porosity, plasma porosity, bulk soil porosity or density, and water content at standard matric potential. A large geographical area of Cambi-Luvisols was sampled at 55 locations with different soil management in western Switzerland. VESS was performed on the pits and layers prior to sampling undisturbed cores. Sandy soils presented medium CoreVESS scores compared to clayey soils. Only soils with more than 20% clay content obtained good scores in this study. The relationships between CoreVESS scores, SOC and most physical properties followed a broken-stick regression, with most breaking points close to score 3. Most regressions were significant and highly determined with R^2 above 0.45. Linear decrease with CoreVESS scores was observed for total porosity and bulk density of air-dried soil and for water content at -10 hPa. The underlying model of structural quality decrease can be summarized as follows. From score 1 to 3 the decrease in structure quality corresponds to a decrease in SOC. From score 1 to 2 occurs most of the decrease in coarse porosity volume. From score 3 to 5 the decrease of structure quality corresponds to a loss of structural porosity, which converges to $0 \text{ cm}^{-3} \text{ g}^{-1}$ for score 5, and to a collapse of the samples upon drying between scores 3 and 4, thus denoting a loss of hydrostructural stability. VESS scores of pits and layers were poorly correlated to CoreVESS scores and physical properties, probably due to local variability of the sampled layers. Our results suggest that the relation between visual scoring and physical properties is not site specific, and underline the need for standardizing the moisture conditions in soil structure quality assessment.

© 2016 Elsevier B.V. All rights reserved.

1. Introduction

Soil structure quality assessments by semi-quantitative visual examination methods using scores, such as VESS (Visual Evaluation of Soil Structure) (Ball et al., 2007; Guimarães et al., 2011) receive increasing attention. Among others, visual examinations can be used to monitor soil quality, to detect

erosion and compaction in cropped fields or to support decision making for tillage practices. They integrate multiple degradation features and processes, are performed directly in the field, do not require extended training, specific equipment or laboratory analyses and the result is immediately available. However visual examinations are considered to be subjective compared to measured physical properties, adding to the fact that they do not address precise physical properties. They are, therefore, unsuitable to quantify structural degradation in physical processes and, for example, to account for structural degradation in the frame of legislation.

Visual examination methods are often compared to different soil physical properties, such as resistance to penetration

* Corresponding author at: University of Applied Sciences and Arts Western Switzerland hepia, Soils and Substrates group, Institute Land-Nature-Environment, Route de Presinge 150, 1254 Jussy Geneva, Switzerland.

E-mail addresses: alice.johannes@hesge.ch, alicejohannes@yahoo.com (A. Johannes).

(Guimarães et al., 2013; Mueller et al., 2009; Newell-Price et al., 2013), flow measurements (Guimarães et al., 2013; Moncada et al., 2015; Pulido Moncada et al., 2014b), aggregate stability (Moncada et al., 2015; Pulido Moncada et al., 2014b), water or air content (Moncada et al., 2015; Mueller et al., 2009), S-index (Moncada et al., 2015) and least limiting water range (Guimarães et al., 2013). Bulk density however, is the most represented property in these comparisons (Table 1). In a large scale study of 30 grassland fields with different soil types, a relation with $R^2 = 0.25$ ($p < 0.01$) was found between visual examinations and bulk density (Newell-Price et al., 2013). Pulido Moncada et al. (2014a) reported a non-linear relationship ($p < 0.01$, $R^2:0.38$) between visual scoring and bulk density in tropical soils from 7 different sites and soil types. Mueller et al. (2009) studied three different sites and soil types and concluded that the relation between bulk density and visual scores were site-specific. On a single field with sandy-loam Cambisol, Pulido Moncada et al. (2014b) found a linear relation with $R^2 = 0.53$ ($p < 0.01$). In another single field of sandy-loam Eutric-Cambisol, Guimarães et al. (2013) found a linear relationship with R^2 up to 0.62 ($p < 0.05$). Therefore, it seems that visual examinations and bulk density are more closely linked when a single soil type is considered. This makes sense because the porosity of the soil is among others determined by texture and type of clay mineral (Boivin et al., 2004; Goutal-Pousse et al., 2016).

Lack of precision is a problem often mentioned not only for visual examinations, but also for physical determinations. Indeed soil physical characterisation is well known to show large variability and unexplained variances (e.g. Horn and Fleige, 2009; Sisson and Wierenga, 1981). This may be due to changing field conditions, especially water content, which is a problem for both visual examinations (Guimarães et al., 2011) and physical measurements (Goutal et al., 2012; Mueller et al., 2009). Shrinkage curve analysis (ShA) provides a good opportunity to help overcome these difficulties, among others because the determined properties show small standard deviations (Boivin, 2007), good correlations with soil constituents (Boivin et al., 2009, 2004) and independence from field water content (Goutal et al., 2012). Therefore ShA receives increasing attention to assess soil compaction or structural changes (Boivin et al., 2006; Fontana et al., 2015; Goutal-Pousse et al., 2016; Peng et al., 2012; Schäffer et al., 2013, 2008). ShA provides a large set of soil physical properties in a single experiment, including bulk density at any

water content. One of the specific features of ShA is that it quantifies separately the volume, the air and water content, and the swelling dynamics of the two soil pores systems, namely the plasma and structural pores. This distinction proved to be important because the two pore systems do not behave the same under compaction (Goutal-Pousse et al., 2016; Schäffer et al., 2013).

Our objective was to characterize and quantify the relationships between soil structure quality scores observed with VESS and physical changes quantified with ShA. To avoid spatial heterogeneity we measured and visually evaluated the same undisturbed sample. Using an adapted method, CoreVESS, we did the evaluations at a standardized soil matric potential. Our samples were collected on the same soil group, namely Cambi-Luvisol, but at large geographical scale, therefore including different textures and soil managements, to establish non-site-specific relations.

2. Material and methods

2.1. Study area – soil characteristics – soil sampling

The study took place across western Switzerland in the cantons of Bern and Vaud, spanning to a distance of 120 km. Samples were randomly collected in spring, summer and autumn from 2012 to 2014 on 55 locations under three different types of soil management, namely permanent grass (14 locations), no-till (24 locations) and plough-based tillage of 20–25 cm depth (17 locations). The sampling covered two textural classes, loam and sandy loam (Food and Agriculture Organization, 2014), and despite large geographical and textural coverage, all the collected samples belonged to the soil type “Braunerde”, according to the Swiss Soil Map (Bundesamt für Landestopographie, 1984), which is intermediate between Cambisols and Luvisols WRB soil groups (Food and Agriculture Organization, 2014). The sampled soils all developed on mixed morain – molasses bed rock. The soil characteristics are presented in Table 2. Undisturbed 5.6 cm diameter soil cores of approximately 150 cm³ were collected at a depth of 5–10 cm at each location, next to the visually evaluated pit (see below). A custom-made sampler was used to allow easy extraction of the undisturbed core from the sampler without disturbing the structure of the sample.

Table 1
Some published relationships between bulk density and visual soil evaluation.

Reference	VSE method	relationship	equation	n	add. info.	rho	R ²	p value
Pulido Moncada et al. (2014b)	VSA	linear	$y = -0.0131x + 1.7266$	12		0.53		<0.01
Pulido Moncada et al. (2014a)	SQSP	logarithmic	$y = -0.199\ln(x) + 1.6094$	36		0.15		<0.05
	VESS		$y = 0.38\ln(x) + 0.9833$	36		0.38		<0.01
	VSA _{mod}		$y = -0.177\ln(x) + 1.9907$	36		0.25		0.01
Garbout et al. (2013)	VESS	linear (Pearson correlation matrix)	NA	8		0.42		<0.05
Newell-Price et al. (2013)	Peerlkamp	NA	NA	30		0.25		<0.01
Guimarães et al. (2013)	VESS	linear	$y = 0.1209x + 0.8865$	30	clayey	0.51		<0.05
			$y = 0.189x + 0.7914$	30	sandy loam	0.62		<0.05
Mueller et al. (2009)	Peerlkamp	monotonic (Spearman rank correlation matrix)	NA	59	Elora site (Canada)	0.56		n.s.
	Diez		NA	59		0.40		n.s.
	VSA – Structure		NA	59		0.58		n.s.
	VSA – Porosity		NA	59		0.63		<0.05
	Peerlkamp		NA	46	Luancheng site	0.02		n.s.
	VSA – Structure		NA	46	(China)	0.77		<0.05
	Werner		NA	46		0.42		n.s.

VSE: visual soil evaluation, VESS: visual evaluation of soil structure, SQSP: soil quality scoring procedure, VSA_{mod}: visual soil assessment (method modified), NA: not available, n: number of observations, add. info.: Additional information, n.s.: not significant, rho: Spearman correlation.

Table 2
Soil characteristics.

	SOC (%)	pH	CEC ($\text{cmol}_c \text{kg}^{-1}$)	Clay < 2 μm (%)	Fine silt 2–20 μm (%)	Coarse silt 20–50 μm (%)	Silt 2–50 μm (%)	Fine sand 50–200 μm (%)	Coarse sand 0.2–2 mm (%)	Sand 0.05–2 mm (%)
mean	1.8	6.5	12.6	19.1	20.9	15.4	36.3	25.5	19.1	44.6
median	1.7	6.4	11.5	18.4	21.4	15.1	36.3	25.3	19.0	45.3
SD	0.6	0.7	5.4	4.2	4.0	4.2	6.8	4.5	7.8	9.1
min	0.8	5.0	5.6	11.6	11.0	7.4	22.6	17.1	5.1	26.3
max	3.7	8.0	27.6	27.9	31.5	25.4	51.7	38.0	34.1	62.4

SOC: soil organic carbon, CEC: cation exchange capacity, SD: standard deviation.

2.2. VESS in the field

VESS (Ball et al., 2007; Guimarães et al., 2011) defines 5 structure quality classes corresponding to scores from 1 (good) to 5 (poor structure). The scoring is done with the help of a chart containing illustrations and descriptions of aggregate shape and size, breaking difficulty, visible porosity and roots. VESS is designed for pits extracted with a spade, where each layer with a different structure is identified and scored separately. The score for the whole pit is finally calculated from the layer scores weighted by each layer thickness. We performed VESS in the field, on 44 out of the 55 locations.

2.3. Analyses

One undisturbed soil sample per location was analysed and the following measurements were performed consecutively on the same sample.

2.3.1. Shrinkage curve analysis (ShA)

The soil samples were removed from the cylinder to swell freely while equilibrating at a matric potential of -10 hPa on a sand table prior to ShA. The samples were then placed in the shrinkage apparatus described in Boivin et al. (2004). Continuous changes in soil height (linear displacement transducer) and mass (weight scale) were recorded every 5 min until height and weight remained constant. The changes in water content were calculated using the recorded weight during analysis and the 105°C oven-dried sample weight after removing the dry mass of the coarse fraction (>2 mm). We measured the sample volumes in the saturated and the air-dried states by the plastic bag method (Boivin et al., 1990) and converted the recorded changes in height to changes in volume after removing the coarse fraction volume as described by Schäffer et al. (2008). This allowed plotting the shrinkage curves, in other words the change in soil specific volume as a function of water content.

The shrinkage curve provides measured physical properties without modelling, and additional properties with modelling. The non-modelled physical properties include soil volume, bulk density, porosity, air and water contents at standardized matric potential, which are therefore independent of field water content and accounting for the shrink-swell properties of the soil. This is meaningful since the change of soil volume with changes in field water content is a problem when comparing bulk densities (Goutal et al., 2012) or bulk density to visual examination (Mueller et al., 2009). For easier comparison with previous studies, we calculated from the specific volume measurements bulk density values (the inverse of specific volume) and total porosity (specific volume minus the solid fraction approximated to $1/2.65 \text{ g cm}^{-3}$). In the following we comment the -10 hPa (wet end of the shrinkage curve) and air-dry soil bulk densities and porosities and the air and water content at -10 hPa. Air content at -10 hPa is the $>150 \mu\text{m}$ equivalent radius porosity according to Jurin-Laplace law and is

referred to as coarse porosity in the following. Water content at -10 hPa is the $<150 \mu\text{m}$ equivalent radius porosity according to Jurin-Laplace law and is referred to as fine porosity in the following. All parameters are reported to one gram of oven dried fine earth (<2 mm fraction).

Shrinkage curves usually exhibit a S-shape (Peng and Horn, 2013), divided in a succession of curvilinear and linear domains separated by transition points (Fig. 1). These elements are often interpreted, from the wet to the dry end of the shrinkage curve, as follows (Braudeau et al., 2004):

- The first linear domain from water saturation to MS point (Fig. 1) is called structural shrinkage and associated to the drainage of structural pores, that is biopores, packing voids and cracks (Brewer, 1964), assumed to allow air entry upon drainage, while plasma is assumed to be at its maximum swelling (MS).
- The second linear domain is called basic or proportional shrinkage. In this domain (from ML point to AE point) full drainage of the structural pores is assumed and the plasma, formed by the soil colloids, i.e. the clay minerals coated with organic matter and oxides (Brewer, 1964), is assumed to shrink like a clay paste without air entry (Sposito, 1973).
- Plasma porosity is the pore space between the colloidal constituents of soil and can also be called textural porosity (Monnier et al., 1973; Peng et al., 2012), matrix porosity (Gerke and van Genuchten, 1993) or intra-aggregate porosity (Gregory et al., 2010). Air entry in the plasma occurs at the end of this domain (AE point, Fig. 1).

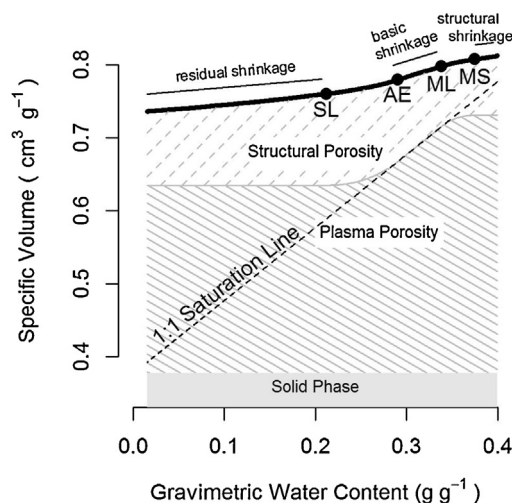


Fig. 1. Example of an experimental shrinkage curve. The saturation line departs water and air in the porosity. Transition points AE (air entry), SL (shrinkage limit), ML (macroporosity limit) and MS (maximum swelling) and residual, basic and structural shrinkage linear domains provided by fitting of the XP model. Structural porosity (dashed crosshatched area) and plasma porosity (crosshatched area) are calculated with XP model.

– The remaining drying and shrinking is called residual shrinkage, which ends with a linear domain from shrinkage limit (SL) to the air-dry soil state (Fig. 1). In the XP model (Braudeau et al., 1999), soil shrinkage is assumed to combine linearly plasma and structural pore shrinkage. Under these assumptions, fitting the XP model allows quantifying the changes of structural and plasma porosities (Braudeau et al., 2004), and the hydro-structural stability of the sample, defined as the ability of the soil to withstand drying forces (Schäffer et al., 2008) and quantified by the slopes of the shrinkage curve. We fitted the XP model (Braudeau et al., 1999) using a full simplex optimisation algorithm (Chen and Saleem, 1986).

Since the structural shrinkage domain is short for these soils (Fig. 1), we focused on the basic shrinkage slope K_{bs} only. Moreover, we considered the plasma and structural porosities at the two extreme transitions points, namely the maximum swelling (MS) and shrinkage limit (SL) points.

2.3.2. CoreVess

To do all the measurements consecutively on the same sample, we adapted the VESS method to be applied on the soil core and propose to call it CoreVess. CoreVess was performed after ShA on each of the 55 undisturbed soil cores, with the following procedure.

The undisturbed soil samples were equilibrated at -100 hPa (field capacity) in a sand box, prior to visual examination. VESS was adapted to small sized cores as follows; two criteria of the VESS method had to be discarded due to the small size of the soil core: (i) the indication on aggregate size over a few centimetres could not be used because it is larger than the sample itself; (ii) rooting, which was considered as not consistent enough to be used as a criteria especially in cultivated soils where the time of sampling is determinant for root density. Finally three criteria which could consistently be observed on all samples were retained: (i) breaking difficulty, (ii) aggregate shape, (iii) visible porosity. A CoreVess score (Sq) from 1 to 5 was given to each sample according to the 3 retained criteria as they are described in the original VESS method. When there was a hesitation between two scores, half points were attributed. Additionally, it must be emphasized that CoreVess was performed as a blind test by two people in order to have an objective evaluation as possible.

After CoreVess, the samples were oven-dried at 105°C , weighted and sieved to 2 mm to determine weight and volume of the coarse fraction (>2 mm). SOC (soil organic carbon content) using the method of Walkley and Black (1934) was analysed on the fine earth of the sample (<2 mm fraction). Texture with the traditional pipette method, water-extract pH and cation exchange capacity using cobalt hexamine chloride (Ciesielski and

Sterckeman, 1997) were determined on fine earth collected next to the sample (Table 2).

2.4. Statistical analysis

Differences between the CoreVess scores were tested with an ANOVA using the “aov” and “TukeyHSD” functions of the R software. Normality was visually controlled with a normal QQ plot and variance homogeneity was controlled with a Fligner-Killeen test. Properties with non-homogeneous variance are not presented in Table 3. Linear regressions between parameters were fitted using the linear model “lm” of the R software (version 3.1.0). In some cases, the relation between the parameters presented two linear parts with changing slopes. Therefore, broken-stick regression (Toms and Lesperance, 2003), graphs and statistics were also fitted using the “segmented” package (version 0.5-1.4) (Muggeo, 2015) of R. Both linear and broken-stick regressions are presented in Fig. 4.

For broken-stick regressions, a simple piecewise-regression model which joins two straight lines at the breakpoint was used.

$$y_i = \begin{cases} \beta_0 + \beta_1 x_i + e_i & \text{for } x_i \leq \alpha \\ \beta_0 + \beta_1 x_i + \beta_2(x_i - \alpha) + e_i & \text{for } x_i > \alpha \end{cases}$$

where y_i is the value for the i th observation, x_i is the corresponding value for the independent variable (here: CoreVess Sq scores), α is the breakpoint and e_i is the additive error. The first slope is β_1 and the second slope is $\beta_1 + \beta_2$, so β_2 can be interpreted as the difference in slopes.

The statistical significance of the breakpoint was given by a Davies test (Davies, 2002), which tests for the difference in slope parameters in a piecewise regression.

3. Results

CoreVess scores were distributed from Sq = 1 to Sq = 4, with one sample at Sq = 4.5. The mean shrinkage curves (Fig. 2) showed a decrease of soil volume and maximum water content (at -10 hPa) with increasing scores (corresponding to a worsening structure). The higher the score, the less difference in specific volumes: between Sq = 3 and Sq = 4, the most noticeable difference was the steeper slope of the shrinkage curve, close to the saturation line for Sq = 4, revealing a general decrease of the hydrostructural stability (weakened structure). This resulted in a much smaller dry specific volume for Sq = 4 than Sq = 3. The mean Sq = 3 and Sq = 4 curves were close to the 1:1 saturation line at the wet end, corresponding to a limited air content. Sq = 4 curves showed the monotonic shape resembling a clay paste, which is typical of structureless soil. The mean total porosity (wet or dry) and bulk density at -10 hPa were significantly different between most scores, except between Sq = 3

Table 3
Difference of average clay, SOC and shrinkage properties between the samples scored from Sq1 to Sq4 with CoreVess.

	Clay	SOC	BD _{dry}	BD _{-10hPa}	P _{dry}	P _{-10hPa}	W _{-10hPa}	A _{-10hPa}	Pl _{MS}	St _{SL}	St _{MS}	K _{bs}
Sq1-Sq2	-5.59	-1.06**	0.16	0.21**	-0.10*	-0.16***	-0.07	-0.09**	-0.03	-0.14**	-0.13**	-0.10
Sq1-Sq3	-8.19**	-1.68***	0.30***	0.38***	-0.17***	-0.27***	-0.15***	-0.11***	-0.09*	-0.18***	-0.17***	-0.22*
Sq1-Sq4	-5.38	-1.48***	0.37***	0.41***	-0.20***	-0.28***	-0.17***	-0.12***	-0.09	-0.23***	-0.19***	0.01
Sq2-Sq3	-2.60	-0.63**	0.14**	0.18***	-0.07**	-0.10***	-0.08***	-0.02	-0.05	-0.05	-0.05	-0.11
Sq2-Sq4	0.21	-0.42	0.21**	0.20*	-0.10*	-0.12*	-0.10*	-0.02	-0.05	-0.09	-0.06	0.12
Sq3-Sq4	2.81	0.20	0.07	0.03	-0.03	-0.02	-0.01	-0.00	0.00	-0.04	-0.02	0.23*

SOC: soil organic carbon, BD_{dry}: air dried soil bulk density, BD_{-10hPa}: bulk density at -10 hPa, P_{dry}: air dried soil porosity, P_{-10hPa}: porosity at -10 hPa, W_{-10hPa}: water content at -10 hPa, A_{-10hPa}: air content at -10 hPa, Pl_{MS}: plasma porosity at maximum swelling, St_{SL}: structural porosity at shrinkage limit, St_{MS}: structural porosity at maximum swelling, K_{bs}: slope of basic shrinkage.

* Tukey test significant at $p < 0.05$.

** Tukey test significant at $p < 0.01$.

*** Tukey test significant at $p < 0.001$.

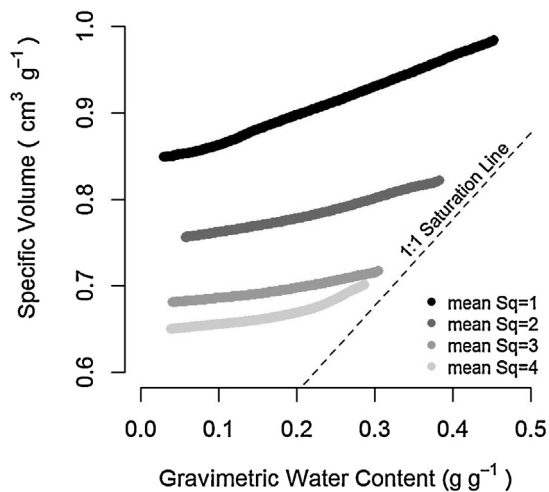


Fig. 2. Average shrinkage curves of the CoreVESS scores from Sq=1 to Sq=4 with the 1:1 saturation line.

and Sq=4 (Table 3). Air-dried soil bulk density and water content at -10 hPa had similar results, but Sq=1 and Sq=2 were not significantly different. Air content and structural porosity could only discriminate Sq=1 from the other scores, while plasma porosity was the same for almost every score (Table 3). Finally the slope of basic shrinkage was the only physical property who could significantly distinguish a moderate structure from a poor structure (Sq=3 and Sq=4) (Table 3), which corresponds to a steeper slope of Sq=4 on Fig. 2. SOC showed significant differences only between the good scores (from Sq=1 to Sq=3) (Table 3).

There was in average no significant difference of clay content among scores, except between Sq=1 and Sq=3 (Table 3). Though the texture ranges differed between scores (Fig. 3). Soils with very good structures (scores from 1 to 1.5) were attributed only to soils with clay content higher than 20% (Fig. 3a), while soils with sand content higher than 50% presented all a moderate structure (scores between 2.5 and 3.5) (Fig. 3b).

Fig. 4 presents the relation between CoreVESS and measured soil properties (SOC and ShA parameters), together with the linear and broken-stick regressions. The parameters of the regressions are presented in Table 4. Significant regressions are plotted with full lines and broken-stick regressions are represented with dashed lines when not significant (Fig. 4). Except air-dried bulk density, air-dried porosity, water content at -10 hPa and plasma pores at maximum swelling (Fig. 4b, d, f), most physical properties did not show a linear relation to CoreVESS and followed the broken-stick model (Fig. 4a, c, e, g, j, k, l). SOC sharply decreased from Sq=1 to

Sq=3, with a breakpoint at a score of 2.68, and stopped decreasing with higher scores than 3, the slope being not significantly different from zero (Fig. 4a). Bulk density at -10 hPa and porosity at -10 hPa also had a break point close to 3 and a slope not different from 0 for larger scores (Fig. 4c, e). The basic shrinkage slope decreased to a breakpoint of 3 but increased after that point (Fig. 4l). While air content at -10 hPa, structural porosity at shrinkage limit and structural porosity at maximum swelling had lower breakpoints of 1.67, 2.07 and 2.24, respectively but were still decreasing after the breakpoints (Fig. 4g, j, k). Finally, the plasma volume at shrinkage limit showed no relation to CoreVESS and was nearly constant (Fig. 4h).

The R^2 of the linear regression models between CoreVESS and physical properties were large and reached up to 0.55 (Table 4). When significant, the adjusted R^2 of the broken stick regression models were always larger. Contrarily, the linear regressions had poor coefficients of correlation when the scores were attributed to the pit or the layer (Table 5), with maximum R^2 of 0.15; broken-stick regression models did not improve it or were not significant. Interestingly, even the linear regression between VESS of the pit or the layer and CoreVESS was very low with R^2 of 0.10 (p 0.038) and 0.11 (p 0.031), respectively.

4. Discussion

4.1. CoreVESS, texture and SOC

Overall, CoreVESS scored different soil structural states and showed well determined relationships to constituents and physical properties. Considering the small standard errors of the ShA parameters (Boivin, 2007), we can assume that the dispersion of the values observed for each score is due to the lower accuracy of semi-quantitative scoring. CoreVESS worked well for soils of different textures, although all textures were not represented on the whole scoring range. The best scores were attributed only to soils with more than 20% clay, while the more sandy soils never received very good or very poor scores (Fig. 3). This is not surprising since clayey soils, which are considered to be more sensitive to compaction, have also a higher potential to form a good, crumbly structure.

The broken-stick regression between SOC and CoreVESS highlights the important role of SOC for physical properties, as often underlined, e.g. by Kay et al. (1997). However, for scores larger than 3, soil structure degradation is not only due to low SOC, since there is no more correlation between scores and SOC for scores above Sq=2.5. In this study, the large scores (Sq \geq 4) were only represented by conventionally tilled fields. Therefore, in addition to low SOC, mechanical stresses are most likely involved in the higher structure degradation.

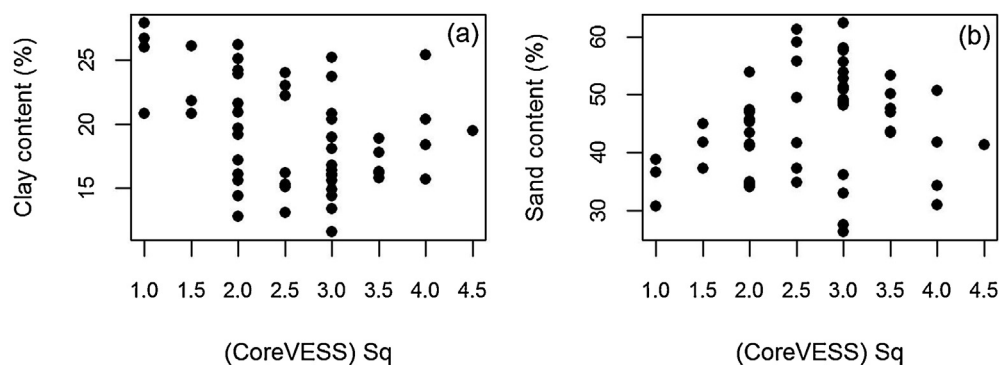


Fig. 3. Clay content (a) and sand content (b) as a function of CoreVESS score (Sq).

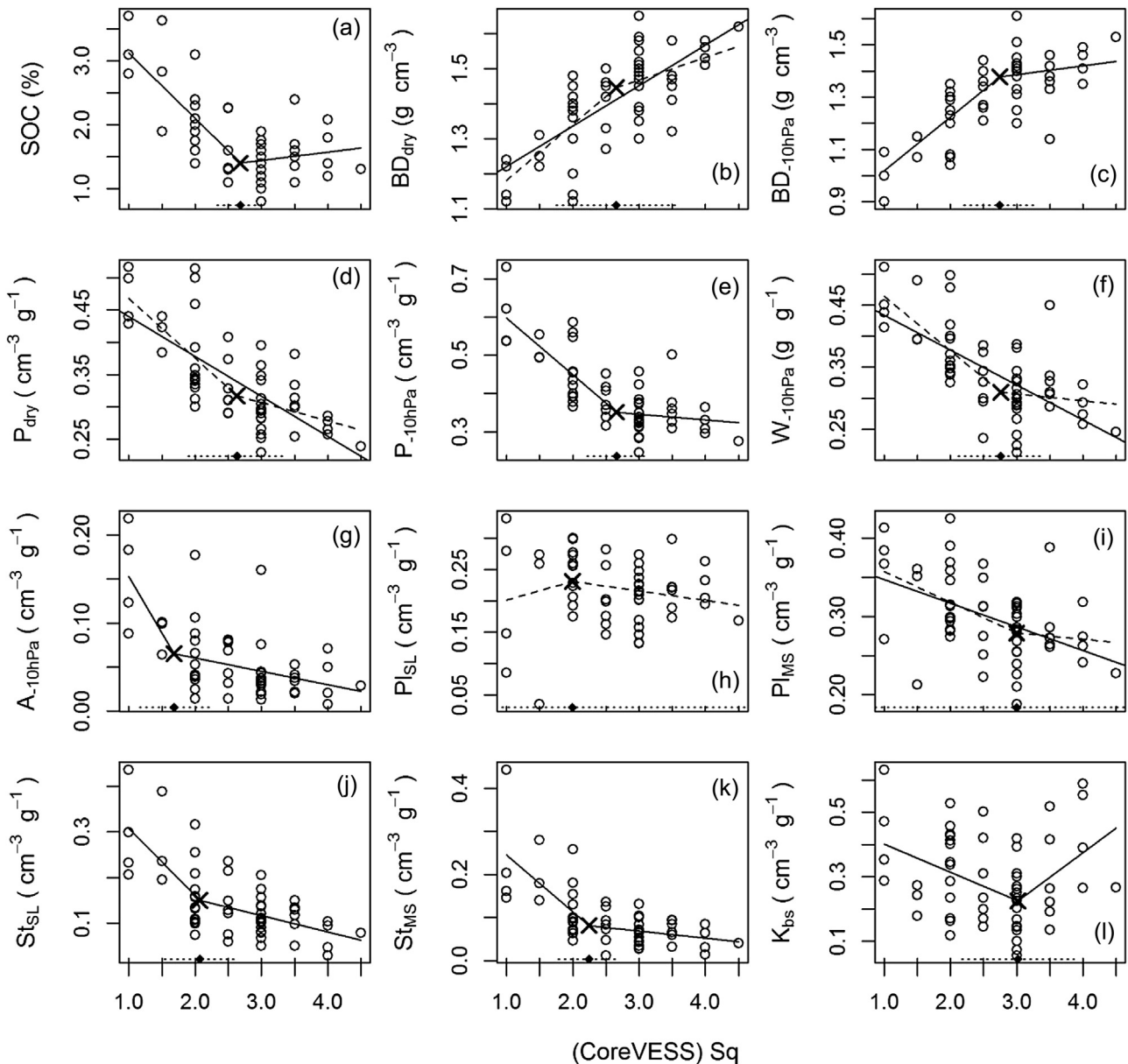


Fig. 4. Soil properties (soil organic carbon (SOC)) (a), air-dried soil bulk density (BD_{dry}) (b), bulk density at -10 hPa (BD_{-10hPa}) (c), air-dried soil porosity (P_{dry}) (d), porosity at -10 hPa (P_{-10hPa}) (e), water content at -10 hPa (W_{-10hPa}) (f), air content at -10 hPa (A_{-10hPa}) (g), plasma porosity at shrinkage limit (Pl_{SL}) (h), plasma porosity at maximum swelling (Pl_{MS}) (i), structural porosity at shrinkage limit (St_{SL}) (j), structural porosity at maximum swelling (St_{MS}) (k) and slope of basic shrinkage (K_{bs}) (l) as a function of CoreVESS scores (Sq). The broken-stick regression is represented in full line when the two slopes are significantly different and in dashed line when they are not. When the broken-stick is not significant but the linear regression is significant, the linear regression is shown. The breakpoint of the broken-stick regression is represented by a cross and the 95% confidence interval appears as a dotted line underneath.

4.2. CoreVESS, shrinkage curve and physical properties

The degradation of the physical properties with increasing scores is comparable to what has been reported in compaction studies (Goutal-Pousse et al., 2016; Peng et al., 2009; Schäffer et al., 2013, 2008). These studies show that with increasing compaction, the soil volume and the maximum water content decrease; the shrinkage curves approach the 1:1 saturation line and show the monotonic shape typical of structureless soils which resembles the shrinkage curve of a clay paste. The steeper and shortened basic shrinkage domain was also reported after high compression (Schäffer et al., 2013), as we observed for the poor structure ($Sq=4$) in Fig. 2.

Coarse porosity is often reported as first impacted by compaction (Alaoui et al., 2011). Accordingly, the volume of

coarse pores sharply decreased from score 1–2. The second remarkable degradation feature is the continuous decrease of total porosity with increasing scores for the air-dry soil, and up to a score of 3 only for total porosity at -10 hPa. This difference between dry and wet soil underlines the importance of moisture conditions. In our case, the volumes are compared at standardized matric potential or swelling state, which is most likely a required condition for such comparisons. The good coefficient of determination between scores and porosities we found supports the assumption of Mueller et al. (2009) that swelling phenomena can jeopardize the quality of soil volume measurements and their correlation to scores. This phenomena can also be observed in another feature distinguishing $Sq=3$ and $Sq=4$, which is the increasing difference between swollen and shrunk soil volume, highlighting the collapse of the weakened

Table 4
Parameters of the regressions between soil properties (SOC, BD_{dry}, BD_{-10hPa}, P_{dry}, P_{-10hPa}, W_{-10hPa}, A_{-10hPa}, Pl_{SL}, Pl_{MS}, St_{SL}, St_{MS} and K_{bs}) and CoreVESS scores. Linear model parameters: Intercept and p-value, Slope and p-value, R². Broken-stick parameters: α: breakpoint with standard error and p-value of Davies test, β₀: intercept and p-value, β₁: first slope and p-value, β₂: the change of slope, 2nd slope (=β₁+β₂) and p value, adjusted R² and R². Bold characters indicate p values significant at level 0.05.

		SOC	BD _{dry}	BD _{-10hPa}	P _{dry}	P _{-10hPa}	W _{-10hPa}	A _{-10hPa}	Pl _{SL}	Pl _{MS}	St _{SL}	St _{MS}	K _{bs}
Linear Model	Intercept	3.15	1.10	0.95	0.50	0.63	0.49	0.14	0.23	0.38	0.31	0.24	0.35
	p value	<0.001	<0.001	<0.001	<0.001	<0.001	<0.001	<0.001	<0.001	<0.001	<0.001	<0.001	<0.001
	Slope	-0.50	0.12	0.13	-0.06	-0.09	-0.06	-0.03	-0.01	-0.03	-0.06	-0.06	-0.02
	p value	<0.001	<0.001	<0.001	<0.001	<0.001	<0.001	<0.001	0.565	<0.001	<0.001	<0.001	0.405
	adj. R ²	0.42	0.53	0.55	0.51	0.54	0.44	0.31	-0.01	0.21	0.41	0.39	-0.01
	R ²	0.43	0.54	0.55	0.52	0.55	0.45	0.32	0.01	0.22	0.42	0.40	0.01
Broken-stick regression	α	2.68	2.68	2.76	2.59	2.64	2.76	1.67	1.96	3.00	2.07	2.24	3.00
	±SE	0.18	0.45	0.27	0.37	0.22	0.32	0.25	1.51	1.20	0.27	0.23	0.28
	Davies p value	<0.001	0.266	0.025	0.121	0.004	0.081	0.006	0.752	0.721	0.031	0.008	0.016
	β ₀	4.15	1.02	0.82	0.56	0.75	0.55	0.28	0.17	0.40	0.46	0.38	0.49
	p value	<0.001	<0.001	<0.001	<0.001	<0.001	<0.001	<0.001	0.123	<0.001	<0.001	<0.001	<0.001
	β ₁	-1.02	0.16	0.20	-0.09	-0.15	-0.09	-0.13	0.03	-0.04	-0.15	-0.13	-0.09
	p value	<0.001	<0.001	<0.001	<0.001	<0.001	<0.001	0.016	0.719	0.001	<0.001	<0.001	0.092
	β ₂	1.15	-0.10	-0.17	0.06	0.13	0.08	0.12	-0.05	0.03	0.11	0.12	0.24
	2nd slope	0.13	0.06	0.03	-0.03	-0.02	-0.01	-0.02	-0.02	-0.01	-0.04	-0.02	0.15
	p value	0.154	0.006	0.229	0.002	0.196	0.435	<0.001	0.011	0.626	<0.001	0.002	0.002
	adj. R ²	0.57	0.54	0.60	0.54	0.62	0.48	0.42	-0.02	0.20	0.47	0.48	0.14
	R ²	0.60	0.56	0.62	0.56	0.64	0.51	0.45	0.03	0.25	0.50	0.51	0.19

SOC: soil organic carbon, BD_{dry}: air dried soil bulk density, BD_{-10hPa}: bulk density at -10 hPa, P_{dry}: air dried soil porosity, P_{-10hPa}: porosity at -10 hPa, W_{-10hPa}: water content at -10 hPa, A_{-10hPa}: air content at -10 hPa, Pl_{SL}: plasma porosity at shrinkage limit, Pl_{MS}: plasma porosity at maximum swelling, St_{SL}: structural porosity at shrinkage limit, St_{MS}: structural porosity at maximum swelling, K_{bs}: slope of basic shrinkage.

Table 5
Parameters of the linear models between VESS scores from the layer and the pits and soil properties. Bold characters indicate p values significant at level 0.05.

		CoreVESS	SOC	BD _{dry}	BD _{-10hPa}	P _{dry}	P _{-10hPa}	W _{-10hPa}	A _{-10hPa}	Pl _{SL}	Pl _{MS}	St _{SL}	St _{MS}	K _{bs}
VESS Layer	Intercept	2.05	2.14	1.32	1.20	0.39	0.47	0.41	0.07	0.23	0.33	0.18	0.13	0.34
	p value	<0.001	<0.001	<0.001	<0.001	<0.001	<0.001	<0.001	0.001	<0.001	<0.001	<0.001	<0.001	<0.001
	Slope	0.27	-0.18	0.04	0.05	-0.02	-0.03	-0.03	0.00	-0.01	-0.02	-0.02	-0.02	-0.02
	p value	0.031	0.057	0.085	0.046	0.083	0.043	0.009	0.705	0.409	0.053	0.204	0.180	0.314
	R ²	0.11	0.08	0.07	0.09	0.07	0.09	0.15	0.00	0.02	0.09	0.04	0.04	0.02
VESS Pit	Intercept	1.68	2.37	1.27	1.13	0.42	0.51	0.44	0.07	0.26	0.36	0.19	0.14	0.32
	p value	0.001	<0.001	<0.001	<0.001	<0.001	<0.001	<0.001	0.017	<0.001	<0.001	<0.001	0.002	0.001
	Slope	0.40	-0.27	0.06	0.07	-0.03	-0.05	-0.04	-0.01	-0.02	-0.03	-0.02	-0.02	-0.01
	p value	0.038	0.075	0.088	0.055	0.084	0.058	0.018	0.633	0.180	0.033	0.306	0.301	0.726
	R ²	0.10	0.07	0.07	0.08	0.07	0.08	0.13	0.01	0.04	0.10	0.02	0.03	0.00

SOC: soil organic carbon, BD_{dry}: air dried soil bulk density, BD_{-10hPa}: bulk density at -10 hPa, P_{dry}: air dried soil porosity, P_{-10hPa}: porosity at -10 hPa, W_{-10hPa}: water content at -10 hPa, A_{-10hPa}: air content at -10 hPa, Pl_{SL}: plasma porosity at shrinkage limit, Pl_{MS}: plasma porosity at maximum swelling, St_{SL}: structural porosity at shrinkage limit, St_{MS}: structural porosity at maximum swelling, K_{bs}: slope of basic shrinkage.

soil structure for Sq=4: The more degraded the structure, the more the soil shrinks with drying, in accordance with the concept of hydrostructural stability proposed by Schäffer et al. (2013). Finally, the last remarkable feature is the structural porosity decreasing down to 0 when extrapolated to Sq=5, with a major decrease taking place between scores 1–3. The loss of total porosity occurs at the expense of structural pores since the dry plasma volume is not changing with scores. The contribution of coarse pores to the decrease of the structural pore volume occurs mostly in the range of scores indicating a good structure, while the continuous decrease down to the higher scores is due to the loss of fine pores.

Fig. 5 presents the underlying conceptual model of gradual loss of soil structure quality: from Sq=1 to Sq=3, total porosity gradually decreases along with SOC. The loss of porosity mostly occurs at the expense of coarse structural porosity from Sq=1 to Sq=2 and of fine structural porosity from Sq=2 to Sq=3. From Sq=3 to maximum degradation, the fine structural pores still decrease in volume and converge to 0 at Sq=5. From Sq=3 to Sq=4, the increase of the basic shrinkage slope corresponds to a gradual structure collapse and loss of hydrostructural stability.

4.3. Threshold degradation score

The broken stick regression model allows quantifying a threshold in structure degradation for most of the soil properties. Non-linear models were used by Pulido Moncada et al. (2014a) to describe the relationship between the visual assessment and the

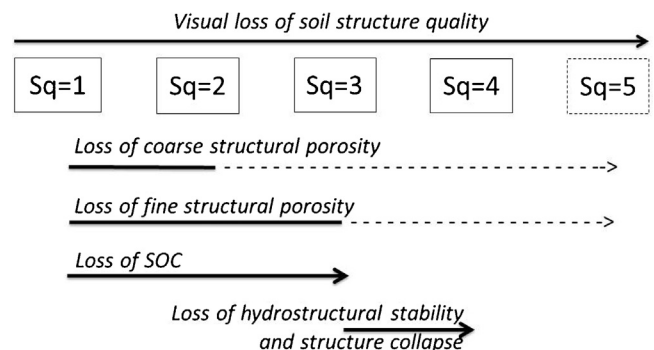


Fig. 5. Conceptual model of soil structure quality loss with increasing scores.

soil physical properties. This is illustrated in their Fig. 3, where a similar threshold can be visually observed for total porosity, bulk density and SOC. Guimarães et al. (2013) studied the least limiting water range which also reached a value of zero for scores of $Sq \geq 3$. Therefore, the thresholds observed in this study are probably a general feature of the VESS scoring. Most break points are close to $Sq = 3$ which is considered by the authors of the VESS method as the limit score, above which soil structure requires improvement, and below which soil structure is considered in an acceptable or even good state. This is supported by our results.

4.4. From field VESS to CoreVESS

The relationship between the measured physical properties and the profile scores was very poor. Even by using the score of the corresponding layer, the relationship did not improve, contrarily to what we expected according to Guimarães et al. (2013). The similar R^2 obtained with pits and layers suggest a large local variability within the layers. Indeed on the field, we observed a large variability of structure at clod scale in pits and layer of the cultivated soils, particularly close to tillage time. Moreover, the undisturbed sample was collected at 10–30 cm away from the pit limit to prevent soil collapse during hammering. Therefore, it was expected that the physical properties of the sampled core be not necessarily representative for the layer score. Nevertheless, when working on the same sample, CoreVESS and measured ShA properties were strongly correlated, similar to what has been found in previous studies within one field, although our study encompassed soils from a large geographical scale, different soil managements and tillage practices. Moreover, because we sampled cropped fields regardless of the season, we sampled different crops at different stages of the management operations. Many factors could explain the residual variance of the regressions, which should be studied at small scale with a single factor changing. The large geographical scale and different soil managements explain the large ranges of clay content and SOC observed. The good relations obtained between the scoring and the physical properties are, therefore, not site specific but rather soil group specific. The sample size we used is common but arbitrary. The purpose was to examine the quality of the relationships between VESS and ShA on the same soil volume, thus preventing a size effect to affect the comparisons. We adapted the VESS criteria that were obviously size dependent, and up scaling of the shrinkage properties is quite well documented. For field relevant characterization, both sample size and local variability must be considered, which was not our objective.

CoreVESS does not give immediate results and requires some simple extra material to be performed. But it improves two reported concerns (e.g. Guimarães et al., 2011) about the field VESS method, namely subjectivity and varying moisture conditions of soil in the field. CoreVESS is practiced as a blind test and the anonymity of the samples implies that the scoring person is not influenced by the surroundings, thus improving objectivity. Most visual examination methods handle subjectivity by having more than one person scoring (Guimarães et al., 2011; Mueller et al., 2009); we think that it is a useful precaution to be taken for CoreVESS as well. Because CoreVESS is done at a standardized matric potential, the comparison between soils is not influenced by different weather conditions during sampling, which would lead to difficulties in comparing aggregate shape or strength. Indeed the physical degradation we observed with ShA was different from wet to dry soil. It is, therefore, preferable to perform field VESS and physical characterizations at standard matric potential for comparison purposes. Although it is possible that soils with different components or texture exhibit slightly different features (e.g. cracking state or aggregate strength) at identical matric

potentials, bringing all the samples at the same matric potential for visual evaluation still seems to be the best and easiest standardization procedure.

According to our results, visual examination is strongly sensitive to structural porosity and structure collapse. This is very encouraging for VESS application, because it makes sense to associate loss of structural porosity to loss of soil quality, since the structural porosity is the biota habitat and accounts for rapid air and water transport. It should be further studied whether the score of the layer takes into account the intra-layer heterogeneity, resulting in an average score of soil structure quality, and whether this could help taking in account local variability for physical measurements.

5. Conclusions

After adaptation of the VESS method to cored soil samples (CoreVESS), the scores of soil structure quality were strongly and significantly related to SOC and various physical properties in a large-scale area. The relationships could be described either by linear or bi-linear (broken-stick) models. In the latter the breakpoint usually occurred around a CoreVESS score of 3, the limit between acceptable and poor structure. Soil texture did not influence the scores, except that the more sandy soils did not receive extreme scores.

Our findings suggest a general model of soil structure degradation under intensive soil management: Decrease in soil porosity is primarily due to by the decrease in structural porosity. Coarse pores are impacted first, leading to an increase in CoreVESS scores from 1 to 2. This increase is associated with a decrease in SOC from score 1–3. At scores higher than 3, SOC remains low. The loss of structural quality between score 3 and 4 is probably due to the mechanical stresses resulting from tillage operations, which lead to loss of hydrostructural stability and structural collapse upon drying.

The relationships between CoreVESS scores and physical properties varied with soil moisture content, highlighting the need to perform visual evaluation and physical measurements at standardised soil moisture conditions. In contrast to the CoreVESS scores, VESS scores determined in situ in soil pits and layers did not yield close relationships with physical soil properties. We attributed this poor relation to local variability.

Acknowledgments

The funding provided by the Swiss federal office of environment for the STRUDEL project (13.001.KP/M044-1527) is gratefully acknowledged. The authors would like to thank Quentin Chappuis for assistance in the laboratory work and Elisabeth Busset for the sampling in the field.

References

- Alaoui, A., Lipiec, J., Gerke, H.H., 2011. A review of the changes in the soil pore system due to soil deformation: a hydrodynamic perspective. *Soil Tillage Res.* 115–116, 1–15. doi:<http://dx.doi.org/10.1016/j.still.2011.06.002>.
- Ball, B.C., Batey, T., Munkholm, L.J., 2007. Field assessment of soil structural quality—a development of the Peerlkamp test. *Soil Use Manag.* 23, 329–337.
- Boivin, P., Brunet, D., Gascuel-Oudou, C., 1990. Densité apparente d'échantillon de sol: méthode de la poche plastique. *Bull. Groupe Fr. Humidimétr. Neutron. Tech. Assoc.* 28, 59–71.
- Boivin, P., Garnier, P., Tessier, D., 2004. Relationship between clay content, clay type and shrinkage properties of soil samples. *Soil Sci. Soc. Am. J.* 68, 1145–1153.
- Boivin, P., Schäffer, B., Temgoua, E., Gratier, M., Steinman, G., 2006. Assessment of soil compaction using soil shrinkage modelling: experimental data and perspectives. *Soil Tillage Res.* 88, 65–79. doi:<http://dx.doi.org/10.1016/j.still.2005.04.008>.
- Boivin, P., Schäffer, B., Sturny, W., 2009. Quantifying the relationship between soil organic carbon and soil physical properties using shrinkage modelling. *Eur. J. Soil Sci.* 60, 265–275. doi:<http://dx.doi.org/10.1111/j.1365-2389.2008.01107.x>.

- Boivin, P., 2007. Anisotropy, cracking, and shrinkage of vertisol samples: Experimental study and shrinkage modeling. *Geoderma* 138, 25–38. doi:<http://dx.doi.org/10.1016/j.geoderma.2006.10.009>.
- Braudeau, E., Costantini, J.M., Bellier, G., Colleuille, H., 1999. New device and method for soil shrinkage curve measurement and characterization. *Soil Sci. Soc. Am. J.* 63, 525–535.
- Braudeau, E., Frangi, J.P., Mohtar, R.H., 2004. Characterizing nonrigid aggregated soil-water medium using its shrinkage curve. *Soil Sci. Soc. Am. J.* 68, 359–370.
- Brewer, R., 1964. *Fabric and Mineral Analysis of Soils*. John Wiley & Sons, New York.
- Bundesamt für Landestopographie, 1984. *Atlas der Schweiz (Böden, Übersicht 7a)*. Chen, D.H., Saleem, Z., 1986. A new simplex procedure for function minimization. *Int. J. Model. Simul.* 6, 81–85.
- Ciesielski, H., Sterckeman, T., 1997. Determination of cation exchange capacity and exchangeable cations in soils by means of cobalt hexamine trichloride. Effects of experimental conditions. *Agronomie* 17, 1–7. doi:<http://dx.doi.org/10.1051/agro:19970101>.
- Davies, R.B., 2002. Hypothesis testing when a nuisance parameter is present only under the alternative: linear model case. *Biometrika* 89, 484–489. doi:<http://dx.doi.org/10.1093/biomet/89.2.484>.
- Fontana, M., Berner, A., Mäder, P., Lamy, F., Boivin, P., 2015. Soil organic carbon and soil bio-physicochemical properties as Co-influenced by tillage treatment. *Soil Sci. Soc. Am. J.* 79, 1435. doi:<http://dx.doi.org/10.2136/sssaj2014.07.0288>.
- Food and Agriculture Organization, 2014. *World Reference Base for Soil Resources 2014 International Soil Classification System for Naming Soils and Creating Legends for Soil Maps*. FAO, Rome.
- Garbout, A., Munkholm, L.J., Hansen, S.B., 2013. Tillage effects on topsoil structural quality assessed using X-ray CT, soil cores and visual soil evaluation. *Soil Tillage Res.* 128, 104–109. doi:<http://dx.doi.org/10.1016/j.still.2012.11.003>.
- Gerke, H.H., van Genuchten, M.T., 1993. A dual-porosity model for simulating the preferential movement of water and solutes in structured porous-media. *Water Resour. Res.* 29, 305–319. doi:<http://dx.doi.org/10.1029/92WR02339>.
- Goutal, N., Boivin, P., Ranger, J., 2012. Assessment of the natural recovery rate of soil specific volume following forest soil compaction. *Soil Sci. Soc. Am. J.* 76, 1426–1435. doi:<http://dx.doi.org/10.2136/sssaj2011.0402>.
- Goutal-Pousse, N., Lamy, F., Ranger, J., Boivin, P., 2016. Structural damage and recovery determined by the colloidal constituents in two forest soils compacted by heavy traffic. *Eur. J. Soil Sci.* 67, 160–172. doi:<http://dx.doi.org/10.1111/ejss.12323>.
- Gregory, A.S., Bird, N.R.A., Whalley, W.R., Matthews, G.P., Young, I.M., 2010. Deformation and shrinkage effects on the soil water release characteristic. *Soil Sci. Soc. Am. J.* 74, 1104. doi:<http://dx.doi.org/10.2136/sssaj2009.0278>.
- Guimarães, R.M.L., Ball, B.C., Tormena, C.A., 2011. Improvements in the visual evaluation of soil structure: visual evaluation of soil structure. *Soil Use Manag.* doi:<http://dx.doi.org/10.1111/j.1475-2743.2011.00354.x> no–no.
- Guimarães, R.M.L., Ball, B.C., Tormena, C.A., Giarola, N.F.B., da Silva, Á.P., 2013. Relating visual evaluation of soil structure to other physical properties in soils of contrasting texture and management. *Soil Tillage Res.* 127, 92–99. doi:<http://dx.doi.org/10.1016/j.still.2012.01.020>.
- Horn, R., Fleige, H., 2009. Risk assessment of subsoil compaction for arable soils in Northwest Germany at farm scale. *Soil Tillage Res.* 102, 201–208. doi:<http://dx.doi.org/10.1016/j.still.2008.07.015>.
- Kay, B.D., Silva, A., da Baldock, J.A., 1997. Sensitivity of soil structure to changes in organic carbon content: predictions using pedotransfer functions. *Can. J. Soil Sci.* 77, 655–667.
- Moncada, M.P., Ball, B.C., Gabriels, D., Lobo, D., Cornelis, W.M., 2015. Evaluation of soil physical quality index S for some tropical and temperate medium-textured soils. *Soil Sci. Soc. Am. J.* 79, 9. doi:<http://dx.doi.org/10.2136/sssaj2014.06.0259>.
- Monnier, G., Stengel, P., Fiès, J.C., 1973. Une méthode de mesure de la densité apparente de petits agglomérats terreux: application à l'analyse de systèmes de porosité du sol. *Ann. Agron.* 24, 533–545.
- Mueller, L., Kay, B.D., Hu, C., Li, Y., Schindler, U., Behrendt, A., Shepherd, T.G., Ball, B.C., 2009. Visual assessment of soil structure: evaluation of methodologies on sites in Canada, China and Germany. *Soil Tillage Res.* 103, 178–187. doi:<http://dx.doi.org/10.1016/j.still.2008.12.015>.
- Muggeo, V.M., 2015. Package segmented. *Biometrika* 58, 525–534.
- Newell-Price, J.P., Whittingham, M.J., Chambers, B.J., Peel, S., 2013. Visual soil evaluation in relation to measured soil physical properties in a survey of grassland soil compaction in England and Wales. *Soil Tillage Res.* 127, 65–73. doi:<http://dx.doi.org/10.1016/j.still.2012.03.003>.
- Peng, X., Horn, R., 2013. Identifying six types of soil shrinkage curves from a large set of experimental data. *Soil Sci. Soc. Am. J.* 77, 372. doi:<http://dx.doi.org/10.2136/sssaj2011.0422>.
- Peng, X., Dörner, J., Zhao, Y., Horn, R., 2009. Shrinkage behaviour of transiently- and constantly-loaded soils and its consequences for soil moisture release. *Eur. J. Soil Sci.* 60, 681–694. doi:<http://dx.doi.org/10.1111/j.1365-2389.2009.01147.x>.
- Peng, X., Zhang, Z.B., Wang, L.L., Gan, L., 2012. Does soil compaction change soil shrinkage behaviour? *Soil Tillage Res.* 125, 89–95. doi:<http://dx.doi.org/10.1016/j.still.2012.04.001>.
- Pulido Moncada, M., Gabriels, D., Lobo, D., Rey, J.C., Cornelis, W.M., 2014a. Visual field assessment of soil structural quality in tropical soils. *Soil Tillage Res.* 139, 8–18. doi:<http://dx.doi.org/10.1016/j.still.2014.01.002>.
- Pulido Moncada, M., Helwig Penning, L., Timm, L.C., Gabriels, D., Cornelis, W.M., 2014b. Visual examinations and soil physical and hydraulic properties for assessing soil structural quality of soils with contrasting textures and land uses. *Soil Tillage Res.* 140, 20–28. doi:<http://dx.doi.org/10.1016/j.still.2014.02.009>.
- Schäffer, B., Schulin, R., Boivin, P., 2008. Changes in shrinkage of restored soil caused by compaction beneath heavy agricultural machinery. *Eur. J. Soil Sci.* 59, 771–783. doi:<http://dx.doi.org/10.1111/j.1365-2389.2008.01024.x>.
- Schäffer, B., Schulin, R., Boivin, P., 2013. Shrinkage properties of repacked soil at different states of uniaxial compression. *Soil Sci. Soc. Am. J.* 77, 1930. doi:<http://dx.doi.org/10.2136/sssaj2013.01.0035>.
- Sisson, J., Wierenga, P., 1981. Spatial variability of steady-state infiltration rates as a stochastic-process. *Soil Sci. Soc. Am. J.* 45, 699–704.
- Sposito, G., 1973. Volume changes in swelling clays. *Soil Sci.* 115, 315–320.
- Toms, J.D., Lesperance, M.L., 2003. Piecewise regression: a tool for identifying ecological thresholds. *Ecology* 84, 2034–2041.
- Walkley, A., Black, I.A., 1934. An examination of the Degtjareff method for determining soil organic matter, and a proposed modification of the chromic acid titration method. *Soil Sci.* 37, 29–38. doi:<http://dx.doi.org/10.1097/00010694-193401000-00003>.